Low-frequency Raman scattering of bioinspired self-assembled diphenylalanine nanotubes/microtubes

Xinglong Wu,[1,*] Shijie Xiong,[1] Minjie Wang,[1] Jiancang Shen,[1] and Paul K. Chu[2]

[1]*National Laboratory of Solid State Microstructures and Department of Physics, Nanjing University, Nanjing 210093, China*
[2]*Department of Physics and Materials Science, City University of Hong Kong, Tat Chee Avenue, Kowloon, Hong Kong, China*
[*]*hkxlwu@nju.edu.cn*

Abstract: Low-frequency Raman scattering from self-assembled bioinspired diphenylalanine (FF) nanotubes/microtubes (NTs/MTs) has been observed for the first time. Four double peaks are identified as the three-dimensional localized collective (acoustic phonon) vibrations of FF molecules in the subnanometer crystalline structure (biological building block) forming the FF NTs/MTs. The increased energy separations between two subpeaks caused by the loss of water in the nanochannel cores are due to the enhancement of vibrational couplings between the FF molecules as a result of the reduction of the influence from water on the coupling. The results provide experimental evidence of localized but still weakly coupled vibrations in organic crystalline nanostructures in the low-frequency region.

©2012 Optical Society of America

OCIS codes: (160.1435) Biomaterials; (300.6450) Spectroscopy, Raman; (120.7280) Vibration analysis.

References and links

1. E. Duval, A. Boukenter, and B. Champagnon, "Vibration eigenmodes and size of microcrystallites in glass-Observation by very-low-frequency Raman-scattering," Phys. Rev. Lett. **56**(19), 2052–2055 (1986).
2. L. Saviot and D. B. Murray, "Long lived acoustic vibrational modes of an embedded nanoparticle," Phys. Rev. Lett. **93**(5), 055506 (2004).
3. A. Courty, A. Mermet, P. A. Albouy, E. Duval, and M. P. Pileni, "Vibrational coherence of self-organized silver nanocrystals in f.c.c. supra-crystals," Nat. Mater. **4**(5), 395–398 (2005).
4. H. K. Yadav, V. Gupta, K. Sreenivas, S. P. Singh, B. Sundarakannan, and R. S. Katiyar, "Low frequency Raman scattering from acoustic phonons confined in ZnO nanoparticles," Phys. Rev. Lett. **97**(8), 085502 (2006).
5. X. L. Wu, S. J. Xiong, Y. M. Yang, J. F. Gong, H. T. Chen, J. Zhu, J. C. Shen, and P. K. Chu, "Nanocrystal-induced line narrowing of surface acoustic phonons in the Raman spectra of embedded Ge_xSi_{1-x} alloy nanocrystals," Phys. Rev. B **78**(16), 165319 (2008).
6. X. L. Wu, S. J. Xiong, L. T. Sun, J. C. Shen, and P. K. Chu, "Low-frequency Raman scattering from nanocrystals caused by coherent excitation of phonons," Small **5**(24), 2823–2826 (2009) (and references therein).
7. M. Reches and E. Gazit, "Casting metal nanowires within discrete self-assembled peptide nanotubes," Science **300**(5619), 625–627 (2003).
8. M. Reches and E. Gazit, "Controlled patterning of aligned self-assembled peptide nanotubes," Nat. Nanotechnol. **1**(3), 195–200 (2006).
9. M. Reches and E. Gazit, "Formation of closed-cage nanostructures by self-assembly of aromatic dipeptides," Nano Lett. **4**(4), 581–585 (2004).
10. N. Kol, L. Adler-Abramovich, D. Barlam, R. Z. Shneck, E. Gazit, and I. Rousso, "Self-assembled peptide nanotubes are uniquely rigid bioinspired supramolecular structures," Nano Lett. **5**(7), 1343–1346 (2005).
11. L. Adler-Abramovich, M. Reches, V. L. Sedman, S. Allen, S. J. B. Tendler, and E. Gazit, "Thermal and chemical stability of diphenylalanine peptide nanotubes: implications for nanotechnological applications," Langmuir **22**(3), 1313–1320 (2006).
12. A. Kholkin, N. Amdursky, I. Bdikin, E. Gazit, and G. Rosenman, "Strong piezoelectricity in bioinspired peptide nanotubes," ACS Nano **4**(2), 610–614 (2010).
13. K. Biswas and C. N. R. Rao, "Nanostructured peptide fibrils formed at the organic-aqueous interface and their use as templates to prepare inorganic nanostructures," ACS Appl. Mater. Interfaces **1**(4), 811–815 (2009).
14. N. Amdursky, M. Molotskii, D. Aronov, L. Adler-Abramovich, E. Gazit, and G. Rosenman, "Blue luminescence based on quantum confinement at peptide nanotubes," Nano Lett. **9**(9), 3111–3115 (2009).

15. N. Amdursky, M. Molotskii, E. Gazit, and G. Rosenman, "Self-assembled bioinspired quantum dots: Optical properties," Appl. Phys. Lett. **94**(26), 261907 (2009).
16. N. Amdursky, E. Gazit, and G. Rosenman, "Quantum confinement in self-assembled bioinspired peptide hydrogels," Adv. Mater. (Deerfield Beach Fla.) **22**(21), 2311–2315 (2010).
17. J. K. Ryu, S. Y. Lim, and C. B. Park, "Photoluminescent peptide nanotubes," Adv. Mater. (Deerfield Beach Fla.) **21**(16), 1577–1581 (2009).
18. C. H. Görbitz, "The structure of nanotubes formed by diphenylalanine, the core recognition motif of Alzheimer's β-amyloid polypeptide," Chem. Commun. (Camb.) (22): 2332–2334 (2006).
19. C. H. Görbitz, "Nanotube formation by hydrophobic dipeptides," Chemistry **7**(23), 5153–5159 (2001).
20. J. B. Kim, T. H. Han, Y. I. Kim, J. S. Park, J. Choi, D. G. Churchill, S. O. Kim, and H. Ihee, "Role of water in directing diphenylalanine assembly into nanotubes and nanowires," Adv. Mater. (Deerfield Beach Fla.) **22**(5), 583–587 (2010).
21. M. J. Wang, S. J. Xiong, X. L. Wu, and P. K. Chu, "Effects of water molecules on photoluminescence from hierarchical peptide nanotubes and water probing capability," Small **7**(19), 2801–2807 (2011).
22. M. J. Frisch, G. W. Trucks, H. B. Schlegel, G. E. Scuseria, M. A. Robb, J. R. Cheeseman, V. G. Zakrzewski, Jr., J. A. Montgomery, R. E. Stratmann, J. C. Burant, S. Dapprich, J. M. Millam, A. D. Daniels, K. N. Kudin, M. C. Strain, Ö. Farkas, J. Tomasi, V. Barone, M. Cossi, R. Cammi, B. Mennucci, C. Pomelli, C. Adamo, S. Clifford, J. Ochterski, G. A. Petersson, P. Y. Ayala, Q. Cui, K. Morokuma, P. Salvador, J. J. Dannenberg, D. K. Malick, A. D. Rabuck, K. Raghavachari, J. B. Foresman, J. Cioslowski, J. V. Ortiz, A. G. Baboul, B. B. Stefanov, G. Liu, A. Liashenko, P. Piskorz, I. Komáromi, R. Gomperts, R. L. Martin, D. J. Fox, T. Keith, M. A. Al-Laham, C. Y. Peng, A. Nanayakkara, M. Challacombe, P. M. W. Gill, B. Johnson, W. Chen, M. W. Wong, J. L. Andres, C. Gonzalez, M. Head-Gordon, E. S. Replogle, and J. A. Pople, *Gaussian 03, Revision A.1* (Gaussian, Inc., Pittsburgh, PA, 2003).
23. J. P. Perdew, K. Burke, and M. Ernzerhof, "Generalized gradient approximation made simple," Phys. Rev. Lett. **77**(18), 3865–3868 (1996).
24. J. B. Foresman, M. Head-Gordon, J. A. Pople, and M. J. Frisch, "Toward a systematic molecular orbital theory for excited states," J. Phys. Chem. **96**(1), 135–149 (1992).
25. C. Peng, P. Y. Ayala, H. B. Schlegel, and M. J. Frisch, "Using redundant internal coordinates to optimize equilibrium geometries and transition states," J. Comput. Chem. **17**(1), 49–56 (1996).
26. R. Krishnan, H. B. Schlegel, and J. A. Pople, "Derivative studies in configuration-interaction theory," J. Chem. Phys. **72**(8), 4654–4655 (1980).
27. A. Komornicki and R. L. Jaffe, "Ab initio investigation of the structure, vibrational frequencies, and intensities of HO_2 and HOCl," J. Chem. Phys. **71**(5), 2150–2155 (1979).
28. X. L. Wu, S. J. Xiong, Z. Liu, J. Chen, J. C. Shen, T. H. Li, P. H. Wu, and P. K. Chu, "Green light stimulates terahertz emission from mesocrystal microspheres," Nat. Nanotechnol. **6**(2), 103–106 (2011).

1. Introduction

Low-frequency (LF) Raman scattering in inorganic nanocrystals (NCs) has been an attractive research subject for the past two decades because of fundamental issues related to the size, shape, surface/interface structure, and confined property of NCs [1–6]. However, for organic molecule crystals which consist of nanoscale molecular building blocks, the collective (acoustic phonon) vibrations of the molecular groups (building blocks) have been seldom studied due to the structural complexity. With the development of self-assembled nanotechnology, studies on the collective vibrations of molecule crystals not only can help to understand the self-assembled growth mechanism, but also provide significant new insights into the physics and chemistry at the atomic/molecular level. Recently, self-assembly of diphenylalanine (L-Phe-L-Phe, FF) molecules, the core recognition motif of the Alzheimer's disease-associated β-amyloid polypeptide, was found to form various stiff as well as chemically and thermally stable nanotubes/microtubes (NTs/MTs) in an aqueous solution [7–13]. These NT/MT structures are expected to have large potential in biochemistry, biomedicine, and molecular sensing in which water weakly bound to FF molecules plays an important role in the biological activity. It was shown that quantum confinement effect that had been observed only from inorganic semiconductor NCs could occur in such self-assembled FF NTs/MTs made of biological building blocks (subnanometer crystalline structures, SCSs) in the form of helices with six FF molecules per turn and side chains emanating from the channel core filled with water molecules [circle, Fig. 1(a)] [14–19]. These SCSs are arranged regularly in the tube walls and have almost the same subnanometer scales, for example, three side lengths of a SCS unit cell $a = b = 2.407$ nm and $c = 0.545$ nm as reported by Gorbitz [18,19]. They form a 3D biological "NC" system which is expected to yield interesting physical effects different from those of inorganic NCs.
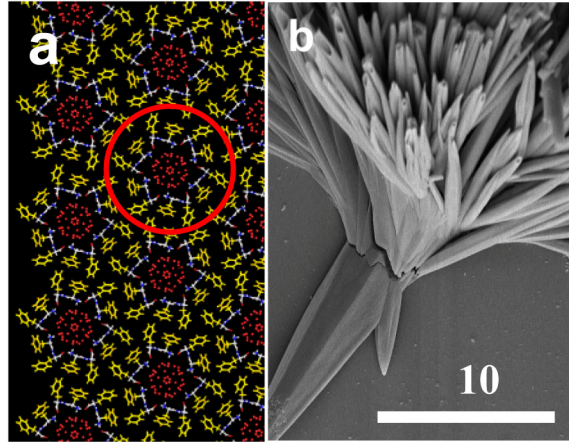
Fig. 1. (a) Locally magnified scheme of FF NT/MT wall consisting of a large number of nanochannel cores. Red circle shows a SCS unit cell in which the weakly combined water molecules (red points) are localized at the center of the channel core. (b) A typical SEM image of the FF NTs/MTs fabricated using a FF concentration of 90 mg/mL at the RH value of 1 and 22 °C.

In this work, LF Raman measurements were conducted on self-assembled hierarchical FF NTs/MTs. Four double peaks are identified as the three-dimensional localized collective (acoustic phonon) vibrations of FF molecules in the SCS (biological building block). The increased energy separation between two subpeaks arises from water loss from the nanochannel cores (less influence of water on the coupling) and enhanced vibrational coupling between the FF molecules. The new results provide experimental evidence of localized but still weakly coupled vibrations in organic crystalline nanostructures in the low-frequency region.

2. Experimental

The humidity-sensitive FF NTs/MTs were prepared by evaporating a drop of fresh FF solution dissolved in 1,1,1,3,3,3-hexafluoro-2-propanol on a glass substrate. The initial concentrations of the FF solutions were varied between 30 and 200 mg/mL and different water vapor pressure values were used in the fabrication by changing the relative humidity (RH) at 22°. The FF solution was dried in 3 min and the FF NTs/MTs were characterized after 30 min.

The LF Raman spectra were acquired at room temperature on a T64000 triple Raman system using a micro-Raman backscattering geometry without a polarization configuration using the 514.5 nm line of an Ar-ion laser as the excitation source. The resolution of the spectrometer was 0.5 cm^{-1}. The diameter of the beam spot was 5 μm and the power was less than 4 mW in order to avoid sample degeneration caused by laser heating. The Raman spectrum acquisition time was 2 min. The high resolution and rejection rate of this measurement system allowed observation of the vibration signals close to the Rayleigh line to less than 5 cm^{-1} [5,6]. The acquired spectra were the same as those taken under excitation by the 488 nm line and no similar LF signals were observed for the used glass substrate.

3. Results and discussion

The scanning electron microscopy (SEM) image of a typical hierarchical FF MT is depicted in Fig. 1(b). The MT has a "feather-like" morphology. Its head is a large MT with a mean diameter of about 3 μm and the tail consists of many small NTs with a diameter of about 360 nm. Clear nanopores can be observed easily and large quantities of SCSs make up the NT/MT walls [18,19].
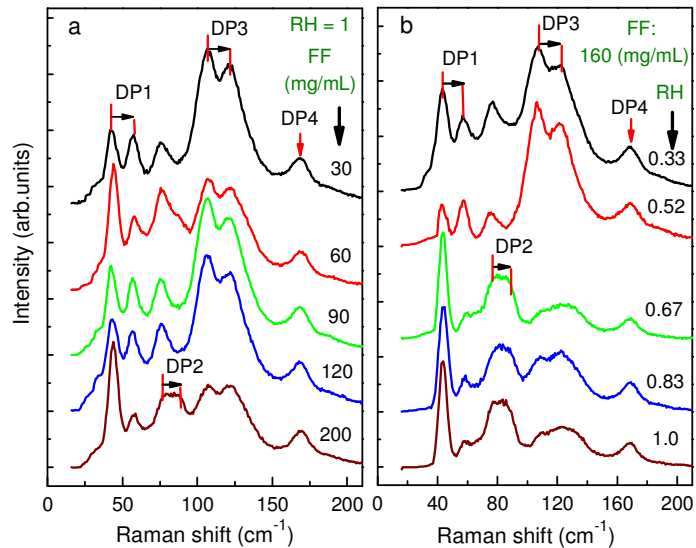
Fig. 2. (a) LF Raman spectra of the FF NT/MT samples fabricated with the FF concentrations ranging from 30 to 200 mg/mL at the RH value of 1. (b) LF Raman spectra of the FF NT/MT samples fabricated with the FF concentration of 160 mg/mL at the RH values varying from 0.33 to 1.0.

Figure 2(a) shows the LF Raman spectra acquired from the FF NT/MT samples with FF concentrations between 30 and 200 mg/mL at RH (relative humidity) of 1. To investigate the LF Raman spectra, we simply divide each one into four paired peaks marked as DP1 at 41.5 and 56.5 cm^{-1}, DP2 at 76.5 and 86.5 cm^{-1}, DP3 at 107 and 122 cm^{-1}, and DP4 due to the dual structure in FF molecule. DP1 and DP3 have the same energy separation of about 15 cm^{-1} and the peak intensity changes with FF concentration. The double-peak structure is pronounced in DP2 produced with an FF concentration of 200 mg/mL. In particular, a relatively small energy separation of ~10 cm^{-1} is observed. The peak observed from DP4 is localized at 168.5 cm^{-1} with a linewidth close to that of DP2. Its position and linewidth do not vary with FF concentration although the intensity varies slightly. For DP4, it is still a double-peak, but cannot be resolved well. Our theory also shows this feature (see below). These spectral features can also be observed from other samples fabricated at different RH values, as shown in Fig. 2(b) that shows the LF Raman spectra of the samples fabricated at an FF concentration of 160 mg/mL and RH values from 0.33 to 1.0. The energy separation between the subpeaks observed from DP1 and DP3 is almost the same whereas that of DP4 still appears at 168.5 cm^{-1}. The only change is that DP2 with a double-peak feature can be observed from the three samples fabricated at RH values of 0.67, 0.83, and 1.0. Hence, it is reasonable to regard DP2 as a paired peak.

To explore the role of water weakly bound to FF molecules via hydrogen bonds in the nanochannel core [20], the LF Raman spectra acquired for different times are presented in Fig. 3. With increasing illumination time (corresponding to more water loss [21]), all the peak intensity is reduced. The energy separation between the two subpeaks also increases for DP2 and DP3. Since the LF modes stem from the collective vibrations of some large molecular groups in the FF molecule, water loss weakens the vibration coupling between these groups with water, leading to strengthening vibration coupling between the large groups themselves, thereby creating significant energy separation between the two subpeaks.
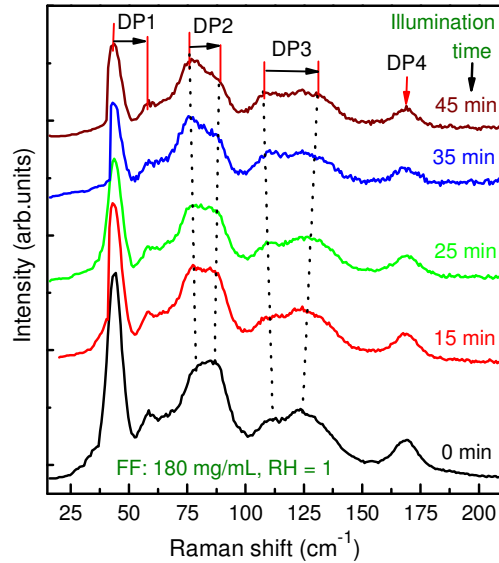
Fig. 3. LF Raman spectra of the FF NT/MT samples with different light illumination times. The initial NT/MT sample was fabricated with the FF concentration of 180 mg/mL at the RH value of 1 and 22 °C.

To theoretically explore the LF vibrations in the FF NT/MT systems, we perform the density-functional-theory (DFT) calculation plus a dynamical matrix scheme to investigate the phonon modes in the LF region. The DFT calculation is carried out with the Gaussian03 code [22] on the collective modes of the FF molecule to specify the positions and directions of the observed LF Raman-active vibrations at the atomic level. The Perdew-Burke-Ernzerh's potential function is adopted in the calculation [23] and geometric optimization is performed by the frozen-core approximation [24,25]. The phonon frequencies and Raman intensities are calculated based on the numerical differentiation of energies obtained from the DFT results [26,27]. There are 8 major Raman-active phonon modes in the frequency range below 180 cm^{-1} and their frequencies, Raman activities, and corresponding displacement vectors are presented in Figs. 4(a)-4(h). All the modes have their corresponding peaks in the measured Raman spectrum as shown in Figs. 2 and 3, with the exception of a small linewidth change and shift to be discussed later in this paper. Owing to the LF nature, these modes are related to vibrations of large groups in the FF molecule. The different modes correspond to different vibration directions and forms thus demonstrating the 3D nature as discussed above. Based on this calculation, vibration details of the peaks observed from the LF Raman spectrum can be investigated.
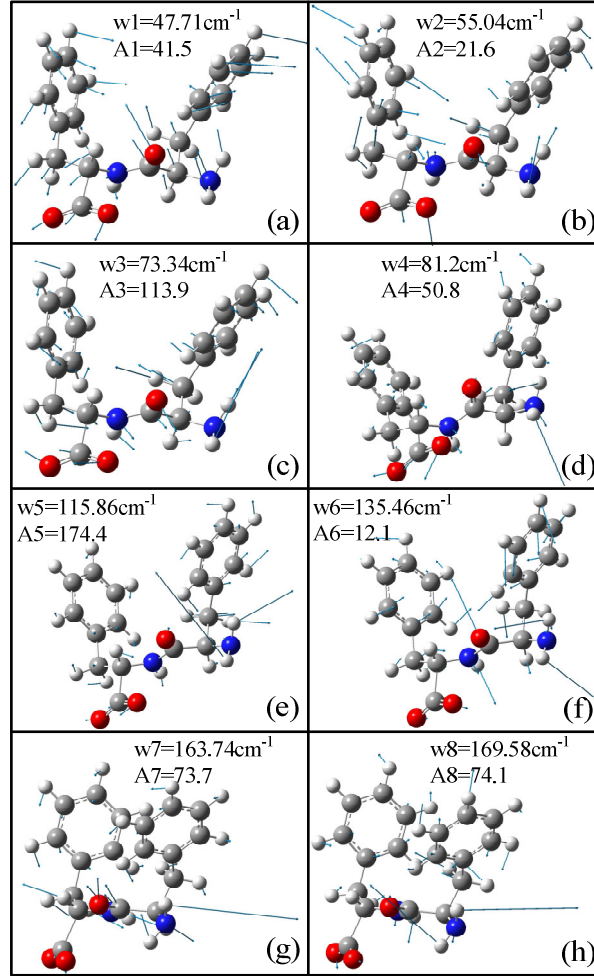
Fig. 4. Displacement vectors of atoms (blue arrows) of the 8 most Raman active modes in the LF range of FF molecule obtained from the DFT calculation. ω_i and A_i with $i = 1,2,...,8$ are corresponding frequencies and Raman activities, respectively.

The localized vibration modes in different FF molecules at the same frequency will couple together producing acoustic waves propagating throughout the whole NT/MT. Since the coupling between different FF molecules is usually very weak, the resulting peak broadening and frequency shifts are also small as shown in Fig. 2. This implies that the coupling between FF molecules mainly occur in a SCS. If we consider a mode ω_i in a FF molecule and pay attention to the nearest neighbor (NN) coupling between FF molecules in the tube, the kinetic energy is

$$K_i = \sum_n \frac{M_i \omega_i^2 X_{in}^2}{2}, \tag{1}$$

where X_{in} is the displacement of the ω_i mode in the nth FF molecule and M_i is the generalized mass corresponding to the ω_i mode in every molecule. The potential energy due to the coupling between molecules is

$$V_i = \frac{1}{2} \sum_{<n,n'>} \lambda_i (X_{in} - X_{in'})^2, \tag{2}$$

where $\langle \ldots \ldots \rangle$ denotes the NN molecules and λ_i is the coupling strength of the NN modes. From the total energy $K_i + V_i$ and dynamic equation for all X_{in}, we can obtain the eigenfrequencies for a nanochannel as [28]

$$\omega_i(k_1, k_2) = \sqrt{\omega_i^2 + \eta_i^2(2 - \cos k_1 - \cos k_2)}, \qquad (3)$$

where $\eta_i = (2\lambda_i/M_i)^{1/2}$, k_1 and k_2 are the wave vectors in the channel direction and plane perpendicular to channel, respectively. Because the channel is formed by a ring of 6 FF molecules in the perpendicular plane (red circle in Fig. 1(a)), k_2 is discretized as $k_{2m} = m\pi/3$ with $m = 0, 1, 2, 3, 4, 5$. We suppose that in the nanochannel direction, the system is infinitely extended and so k_1 is continuous in the range of $[0, 2\pi]$. Considering the different Raman activities of the modes, the whole Raman spectrum can be calculated as

$$I(\omega) = \sum_{i=1}^{8} \sum_{m=0}^{5} A_i \int_0^{2\pi} \delta\left[\omega - \omega_i(k_1, k_{2m})\right] dk_1, \qquad (4)$$

where A_i is the Raman activity for mode ω_i obtained in the above DFT calculation for a single FF molecule.
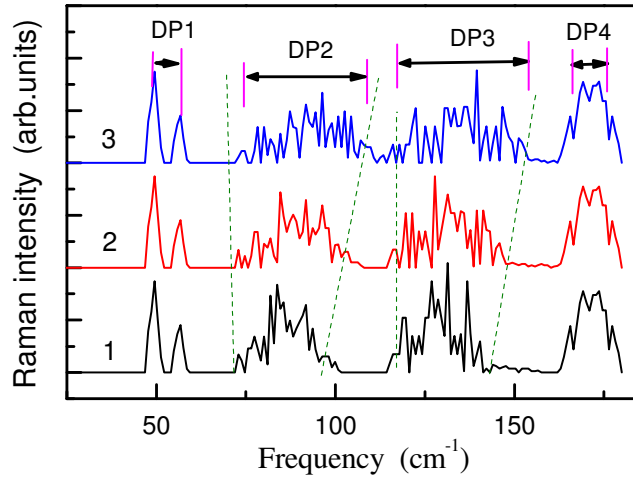

Fig. 5. Calculated Raman intensity in the LF range of a SCS. ω_i and A_i with $i = 1,2,\ldots,8$ are obtained from the DFT calculation for FF molecule. Other parameters are selected in a SCS as: $\eta_1 = \eta_2 = 10$ cm^{-1}, $\eta_7 = \eta_8 = 30$ cm^{-1}. For black curve 1: $\eta_3 = \eta_4 = 30$ cm^{-1}, $\eta_5 = \eta_6 = 40$ cm^{-1}. For red curve 2: $\eta_3 = \eta_4 = 35$ cm^{-1}, $\eta_5 = \eta_6 = 45$ cm^{-1}. For blue curve 3: $\eta_3 = \eta_4 = 40$ cm^{-1}, $\eta_5 = \eta_6 = 50$ cm^{-1}.

According to the above analysis, we can expect that due to the coupling between FF molecules, the discrete LF phonon modes in one FF molecule should be extended to bands with widths depending on the size of the SCS. Such a reformation is determined by the values of η_i which may be affected by water molecules in the SCS core. Figures 2 and 3 show that $\omega_{1,2,7,8}$ (DP1 and DP4) has a smaller linewidth change with FF concentration, RH, and amount of water in the nanochannel than ω_{3-6} (DP2 and DP3). Hence, we only consider the influence of water molecules on η_{3-6}. Figure 5 plots the calculated Raman intensity for different values of η_{3-6} in a SCS. The curves reproduce the behavior of the measured Raman spectrum depicted in Fig. 3. DP1 and DP4 show almost the same linewidths and line shape, but not DP2 and DP3. This indicates that the acoustic vibrations of a SCS determine the LF Raman scattering. The samples under longer optical radiation yield larger coupling strength η_{3-6}. This is because under radiation, water molecules escape and their effects on the coupling between FF molecules is reduced. Consequently, the coupling strength is increased. The enhanced coupling also widens the bands and reduces the peak heights. This coupling change caused by

water addition and loss changes the SCS sizes and it has been confirmed by our DFT calculation and x-ray diffraction [21].

4. Conclusion

Four double peaks are observed from LF Raman spectra acquired from self-assembled bioinspired FF NTs/MTs. As water is lost from the nanochannel cores, the relative peak intensity diminishes and the separation between the double peak increases. DFT calculation reveals that the observed peaks stem from 3D collective vibrations of FF molecules in the SCS. The loss of water molecules decreases significantly the effects of water on the coupling between FF molecules. Consequently, the band width and energy separation increase. Our results provide for the first time evidence of local collective vibrations in inorganic NC systems.

Acknowledgments